25th ABCM International Congress of Mechanical Engineering
October 20-25, 2019, Uberlândia, MG, Brazil

COB-2019-1186
TEST BENCH FOR THE DEVELOPMENT OF IMAGING RECONSTRUCTION ALGORITHMS OF THE ULTRASOUND TOMOGRAPHY

Nilton Barbosa da Rosa Júnior
Chi-Nan Pai
Polytechnic School of the University of Sao Paulo, Department of Mechatronic and Mechanical Systems Engineering, Sao Paulo, Brazil.
nilton.rosa.jr@usp.br, chinan.pai@usp.br

Abstract. *A real-time and continuous imaging method is important to monitor patients under mechanical ventilation in the intensive care unit. Conventional ultrasound imaging requires an operator to position the probe, while the Electrical Impedance Tomography presents low spatial resolution and low location accuracy. The Ultrasound Tomography (UST) has the potential to provide better pulmonary functional imaging. However, it has never been used before. The objective of this work is to develop an experimental test bench, to simulate a UST, to evaluate its feasibility for pulmonary functional imaging, and to develop imaging reconstruction algorithms. Eight mono-element transducers were manufactured by using 500 kHz piezoelectric ceramic and were characterized by measuring its electrical impedance and by using the pulse-echo technique. The transducers were assembled on a wooden cylinder that was placed inside a tank filled with water. One transducer was used as emitter and four others as receptors, with a phantom placed in several positions inside. The electrical impedance and the pulse-echo results showed frequencies below 200 kHz with amplitudes between 20 and 300 mV (peak-to-peak), adequate for lung imaging. The evaluation of the test bench also showed signals compatible with expected, showing the feasibility of the UST.*

Keywords: *Ultrasound tomography, PZT transducer, Lung monitoring, Mechanical ventilation*

1. INTRODUCTION

Patients with severe respiratory disease frequently need mechanical ventilation (MV) to provide enough oxygenation of the blood. These patients require a close evaluation of their lung function for adequate adjustment of the ventilator and to avoid possible related barotrauma, which is likely to happen in patients with acute respiratory distress syndrome and chronic obstructive pulmonary disease (Polese et al., 2005). Thus, in order to reduce the occurrence of barotrauma, parameters in the MV must be adjusted according to the clinical condition of each patient.

Methods that are available for assessing lung function in patients in Intensive Care Unit (ICU) under MV include: arterial blood gas analysis and graphic waveforms from ventilators (flow and pressure). Nevertheless, these methods reflect only overall lung function, failing to provide information on localized functionality, such as proper ventilation of parts of the lung, which is important to adjust the parameters of MV (Cinel et al., 2007). Hence, an alternative that can be used for localized assessment of the lung function is through imaging exam.

Pulmonary functional imaging is one of the most important exams to avoid barotrauma, because it can monitor the ventilation and the perfusion of the lung in real time (Chiumello et al., 2013). The conventional ultrasound and Electrical Impedance Tomography (EIT) are options for pulmonary functional imaging. These exams are non-invasive, available at the bed-side and can provide real-time and continuous images of the lung due to the absence of ionizing radiation (Ball et al., 2017).

Although conventional ultrasound is widely exploited in medical environment, this exam depends on an operator to position the ultrasound probe to the region of interest. Therefore, it is unfeasible for use as a long-term monitoring device. EIT is another option for pulmonary functional imaging (Chiumello et al., 2013). It can generate a real-time functional imaging of lungs during continuous application of MV, allowing the identification of an optimal Positive-End Expiratory Pressure for MV (Nieman et al., 2017). However, the EIT imaging suffers from low spatial resolution and low location accuracy compared to conventional ultrasound imaging (Steiner et al, 2008).

Our group is investigating the possibilities to use Ultrasound Tomography (UST) as a new and innovative imaging method for monitoring the lung function of patients under MV. In ultrasound imaging measurements, the amplitude of the ultrasound wave and its time of flight are available for imaging reconstruction algorithms. Therefore, it has the potential to provide more information for lung functional monitoring than EIT imaging.

Despite applications for breast imaging, UST has never been used to monitor the lungs, because it is a very challenging task, considering that, during the inspiration, the lungs would be full of air, which represents a high acoustic impedance medium. However, Rueter et al. (2009) proved that for non-invasive lung monitoring with ultrasound, a central frequency lower than 750 kHz would be able to pass through the entire thoracic wall. Besides, Song et al. (2018) showed that it is feasible to use low frequency ultrasound for human thorax imaging. Hence, using ultrasound can be a new method for continuous non-invasive lung imaging in ICUs with patients under MV.

In order to develop a novel UST system for lung monitoring, both hardware and software must be researched; the hardware is composed of drives, acquisition system and transducers while the software is composed of digital filters and imaging reconstruction algorithms. The development of imaging reconstruction algorithms requires a well-known environment to estimate the imaging reconstruction error. Therefore, test bench for UST can be used as an approach to understand the problem of reconstruction imaging, estimate errors and to validate the entire system before its application in clinical environment (Liu et al., 2018).

In the present work an experimental test bench that simulates an UST system for lung monitoring is developed. It will be possible to change the domain of this test bench in order to test the imaging algorithms, so that we can evaluate the feasibility of this technology as a new modality of pulmonary functional imaging, develop imaging reconstruction algorithms, and understand this new technology for the development of a prototype of UST for clinical use.

2. MATERIALS AND METHODS

2.1 Manufacturing process of the transducers and the test bench

Figure 1 (a) shows a schematic of the UST test bench, which consists of a wooden cylinder, on which eight mono-element Lead Zirconate Titanate (PZT) transducers are fixed. The transducers were symmetrically attached on the wooden cylinder by U clamps. The distance between the frontal face of two opposite transducers was 300 mm, which is the mean diameter of the human thorax. The wooden cylinder was waterproofed by wood sealer and marine varnish and fixed on an aluminum base.

Figure 1 (b) shows a schematic of the mono-element transducer. A PZT ceramic, (DL50, Delpiezo Inc., U.S.A.) with central frequency of 500 kHz, was placed inside a silicone tube, to avoid short circuit between the electrodes for signal and for ground, and a backing layer is placed on the backside of the ceramic, inside the silicone tube. This resonance frequency was used because ultrasound waves below 750 kHz were shown to be able to pass through the thorax (Rueter et al., 2009; Song et al., 2018).

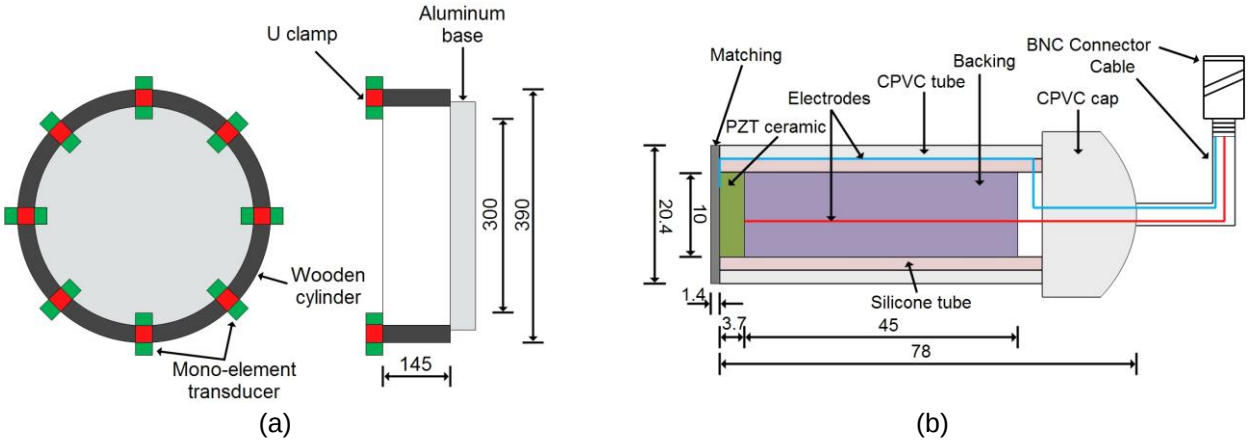

Figure 1: (a) schematic of the test bench developed and (b) a mono-element transducer. Units are in millimeters.

The silicone tube was inserted into a Chlorinated Polyvinyl Chloride (CPVC) tube, used as the transducer housing. The electrodes were welded on both faces of the PZT ceramic and connected to a Bayonet Neill–Concelman (BNC) connector. Silicone glue was used to fix CPVC cap to CPVC tube, and to waterproof the entire transducer.

The backing layer was made from tungsten powder and a mixture of epoxy resin and its hardener (SQ2001 and SQ3154, 2:1). The proportion of tungsten with respect to epoxy was 30% in mass, resulting in attenuation of 0.913 dB/cm for a frequency of 500 kHz (Coelho; Pai, 2017). Therefore, its thickness was 45 mm. The matching layer was made from the mixture of epoxy resin and its hardener (SQ2001 and SQ3154, 2:1) with 30% in volume of alumina dust, and its thickness is approximately 1.4 mm.

2.2 Evaluation of the transducers and the test bench

The characterization of the transducers was made through an impedance analyzer (4294A, Agilent, USA) and Pulse-Echo technique. The electrical impedance of the PZT ceramics and the manufactured transducers were measured, allowing the analysis of changes in the transducer responses, and also for the design of the electronics for driver and receiver in the future.

Each manufactured transducer was immersed in a water tank with a reflector positioned at a distance of 98 mm from the transducer. A pulser (5077PR, Olympus, Japan) drives the transducer with a square wave [amplitude (peak-to-peak) of 100 V_{pp}, pulse width of 4 μs and repetition time of 10 ms]. Then, the echo signal of each transducer was recorded by an oscilloscope (DSO3102A, Agilent, USA) and processed in Matlab to obtain the maximum V_{pp} and the resonance frequency.

The test bench was placed in a tank filled with water, as shown in Fig. 2 (a). A cylindrical phantom, which was made from the mixture of epoxy resin (ARALDITE GY 260) and 20% in volume of its hardener (ARADUR HY 956), was hanged between transducers by strings, which are fixed on a bar placed on the top side of the tank. Thus, the phantom could be placed at different positions inside the test bench.

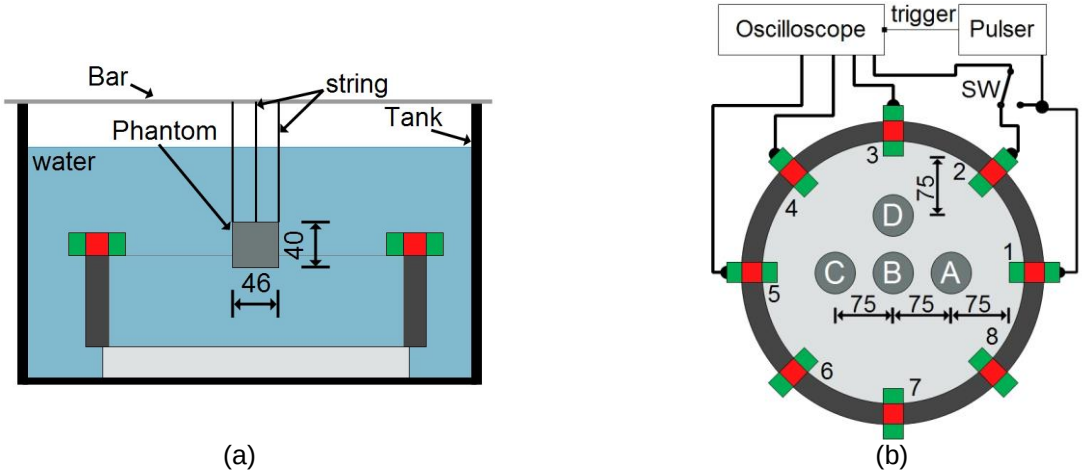

Figure 2: (a) test bench placed in a tank filled with water, and (b) a schematic of the complete system to transmit and receive signals for UST test bench. Units are in millimeters.

Figure 2 (b) illustrates the test bench assembly with eight mono-element transducers. The phantom was placed at four positions (A to D), so that different signals could be recorded and analyzed. Also, T1 was used as emitter whereas the other four transducers as receivers.

Due to the symmetry, only transducers (T1-T5) were used in the evaluation, due to the fact that if the phantom were placed in front of T7, the signal pattern of (T6-T8) would be similar to (T2-T4) signal, with the phantom placed at position D. Thus, only half of the test bench was used to record the signals.

The same pulser generated a trigger signal to synchronize the oscilloscope (MSO8104A, Agilent, USA) and drived the T1 with a square pulse of 100 V_{pp}, width of 2.87 μs, and repetition time of 10 ms, whereas the oscilloscope recorded the signals that were received by the other transducers. In the Fig. 2 (b), SW represents the connection of the oscilloscope channel that is used to record the pulsed signal that drives the T1, or to record the signal of the T2.

3. RESULTS

Figure 3 (a) shows the manufactured transducer and its dimension and Fig. 3 (b) illustrates the manufactured test bench placed inside the tank filled with water. Fig. 4 (a) shows the electrical impedance of the DL50 PZT ceramic and the final electrical impedance of transducer 1, which operates as emitter, while Fig. 4 (b) illustrates the electrical impedance of the DL50 PZT ceramic and the final electrical impedance of transducer 5, which operates as receiver. The amplitude measured in ohm of the electrical impedances were divided by 1 and converted to decibel (dB). All other manufactured transducers have similar electrical impedance measurement.

Comparing the electrical impedance of transducer 1 and DL50 ceramic (Fig. 4 (a)), the electrical impedance of the DL50 ceramic contains other resonance frequencies, 188 kHz, 344 kHz, and 573 kHz, with the central frequency of the PZT ceramic being 491 kHz. These other frequencies are related to other vibration modes, which are determined by the geometry of the ceramic, depending on its thickness and diameter.

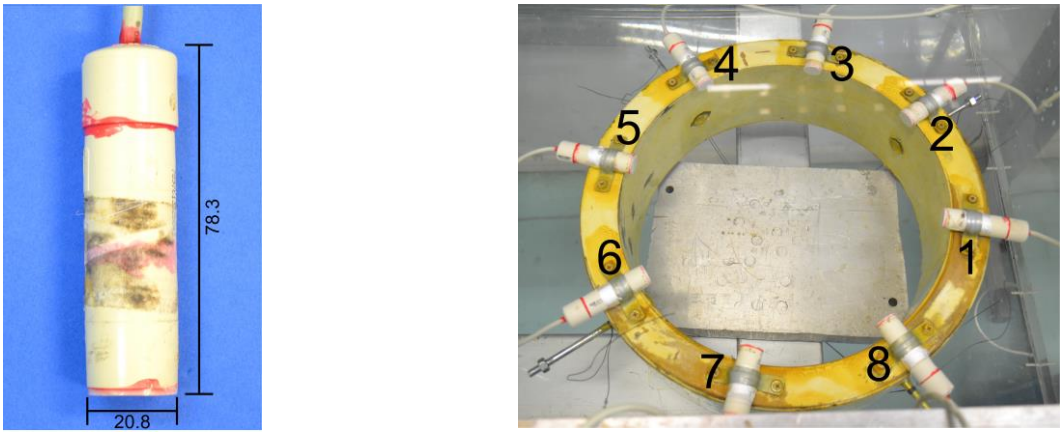

(a) (b)

Figure 3: (a) Manufactured transducer and (b) the test bench. Units in millimeters.

In this case, the radial mode (188 kHz) is more predominant than the axial mode of vibration (491 kHz), because the ratio (diameter/thickness) of the PZT ceramic is lower than 20 (Kunkel, H. et al., 1990). Besides, when the backing was added to the PZT ceramic, it dumped the axial mode but had no influence on the radial mode of vibration. Thus, analyzing the electrical impedance of the transducer 1, only the low frequency vibration mode at 177 kHz is visible, and the same occurs to the other transducers.

This frequency is lower than the expected 500 kHz. Nevertheless, for development of UST for lung monitoring, it is an advantage, because lower frequency is preferred (Rueter et al., 2009; Song et al., 2018). Therefore, the manufactured transducers are better than expected; Fig. 4 (c) shows the maximum amplitude V_{PP} and resonance frequency from each transducer, respectively.

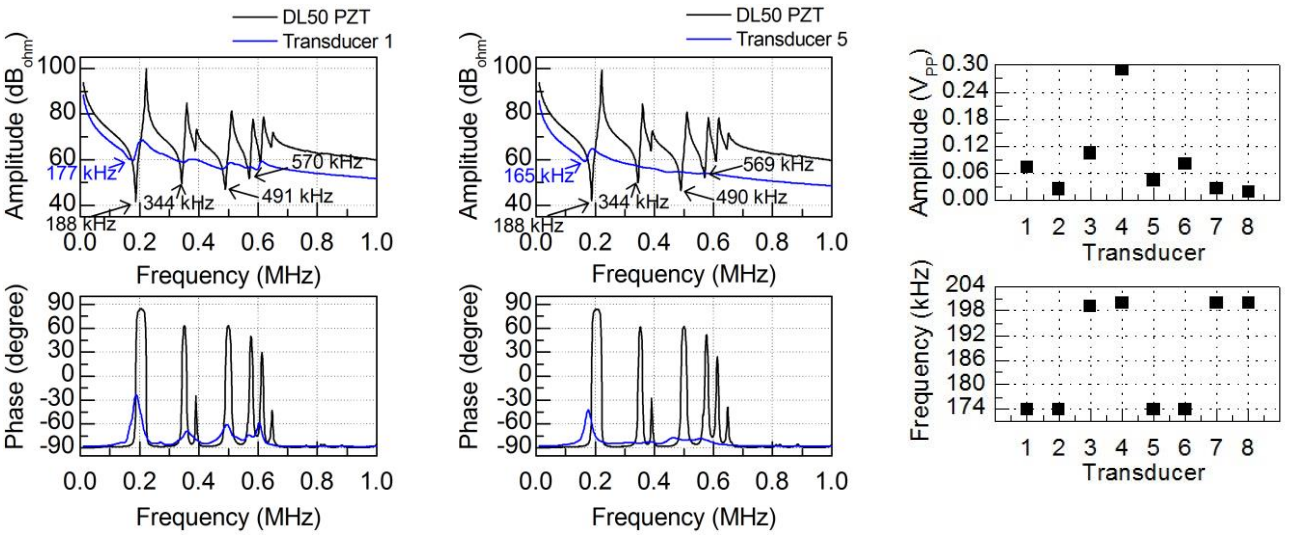

(a) (b) (c)

Figure 4: (a) Electrical impedance of PZT ceramic and transducer 1, (b) electrical impedance of PZT ceramic and transducer 5, and (c) the maximum amplitude V_{PP} and resonance frequency of each transducer.

Figure (5 to 9) illustrate the measured signals of the transducer 2 (T2), the transducer 3 (T3), the transducer 4 (T4) and the transducer 5 (T5), and the pulse generated by the pulser to drive the transducer 1 (T1), for the phantom placed at the positions A, B, C and D. Moreover, signals were recorded with no phantom placed inside the test bench. There is a schematic showing the position of the emitter, the receiver and the phantom on the bottom left corner of each figure.

Analyzing only the signal T5 with no phantom (Fig. 5), multiple peaks (1, 2 and 3) can be seen. It happens because of the signal reflections on the surface of the wooden cylinder and water-air interface, due to the spread of the transducer beam; these multiple peaks are present in T2, T3 and T4 as well. Therefore, considering that the thoracic wall will also reflect the ultrasound waves, a real situation was well simulated by the manufactured UST test bench.

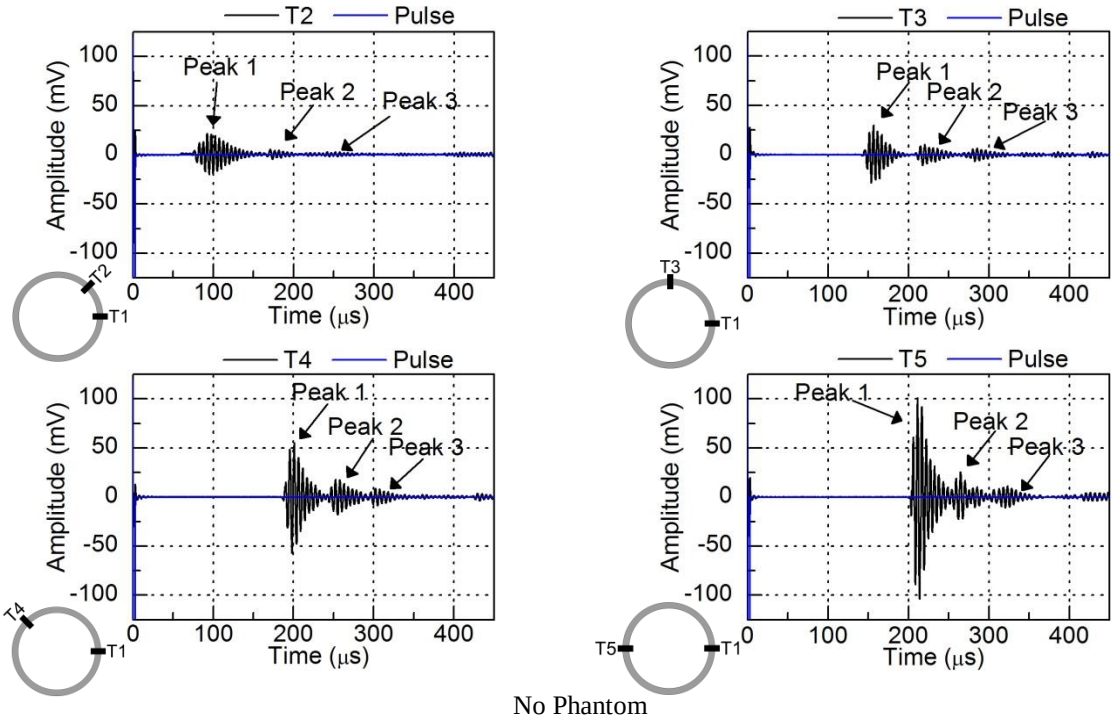

Figure 5: Recorded signals with no phantom placed inside the test bench.

Figure 6 shows the measured signals of T2, T3, T4 and T5, and the pulse generated by the pulser to drive the T1. The amplitude of T5, when the phantom is placed at position A, is smaller than its amplitude with no phantom, indicating that the signal passed throughout the phantom. Comparing the results between the Fig. 4 and 5, it can be seen that there is no change in signal amplitude for the first peak of T2, T3 and T4. Therefore, practically, the signals T2, T3, and T4 suffered no influence of the presence of the phantom at positions A.

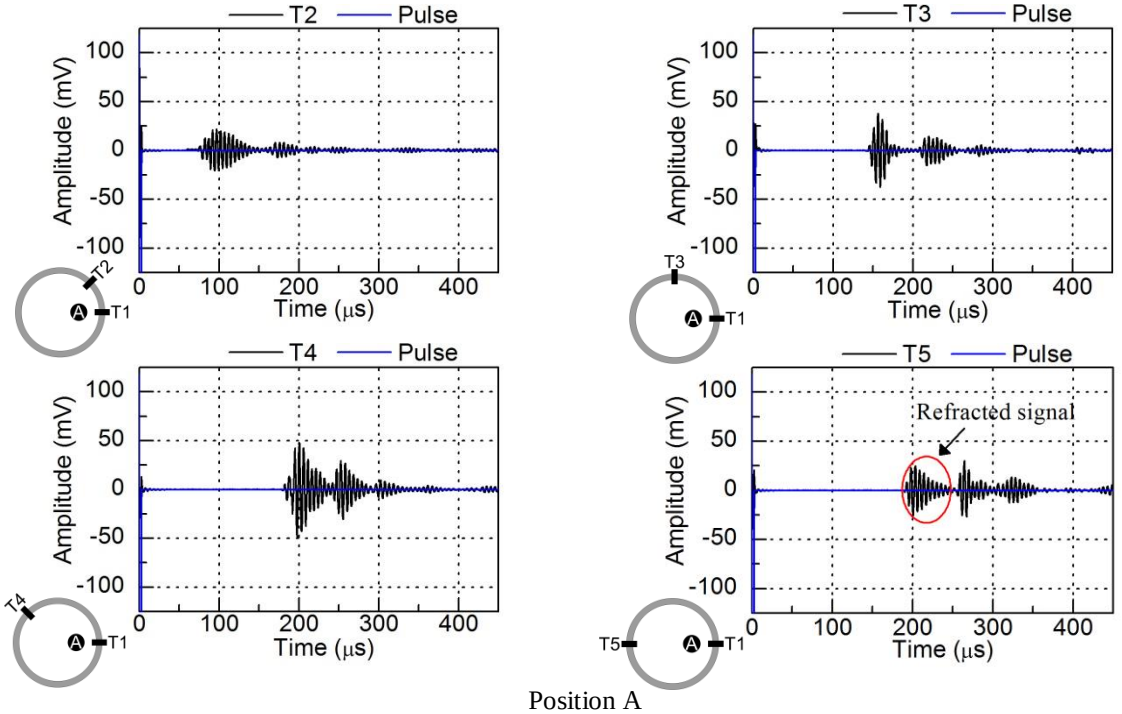

Figure 6: Recorded signals with phantom at position A.

Figure 7 illustrates the measured signals when the phantom is placed at position B. Here, the amplitude of T2, T4 and T5 signals remains almost the same. But, in T3 signal is possible to see the presence of a reflected signal from the

phantom. This reflected signal was not present when the phantom was placed at position A, thereby moving the phantom inside the test bench can be detected by the transducers.

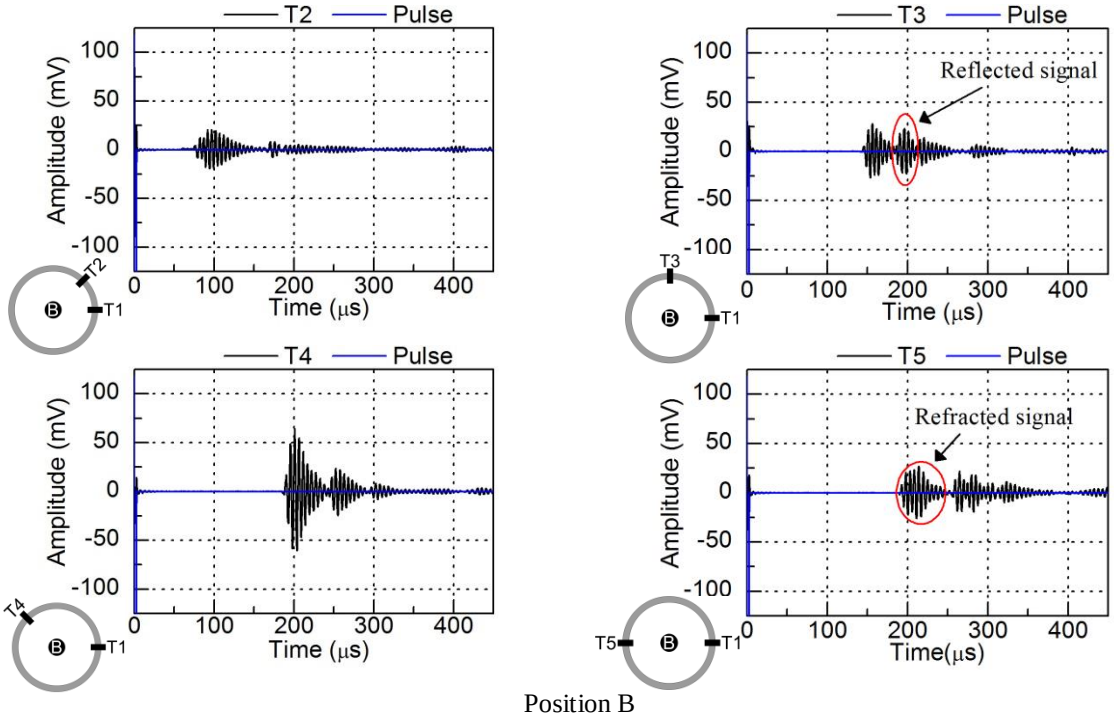

Position B

Figure 7: Recorded signals with phantom at position B.

After changing the position of the phantom to C (Fig. 8), the reflected signal is not present in T3 signal anymore. For this configuration, the signal patterns are similar to the ones previously presented when the phantom was placed at position A (Fig. 6). Yet, a refracted signal can be seen in T5 because the phantom is placed between T1 and T5.

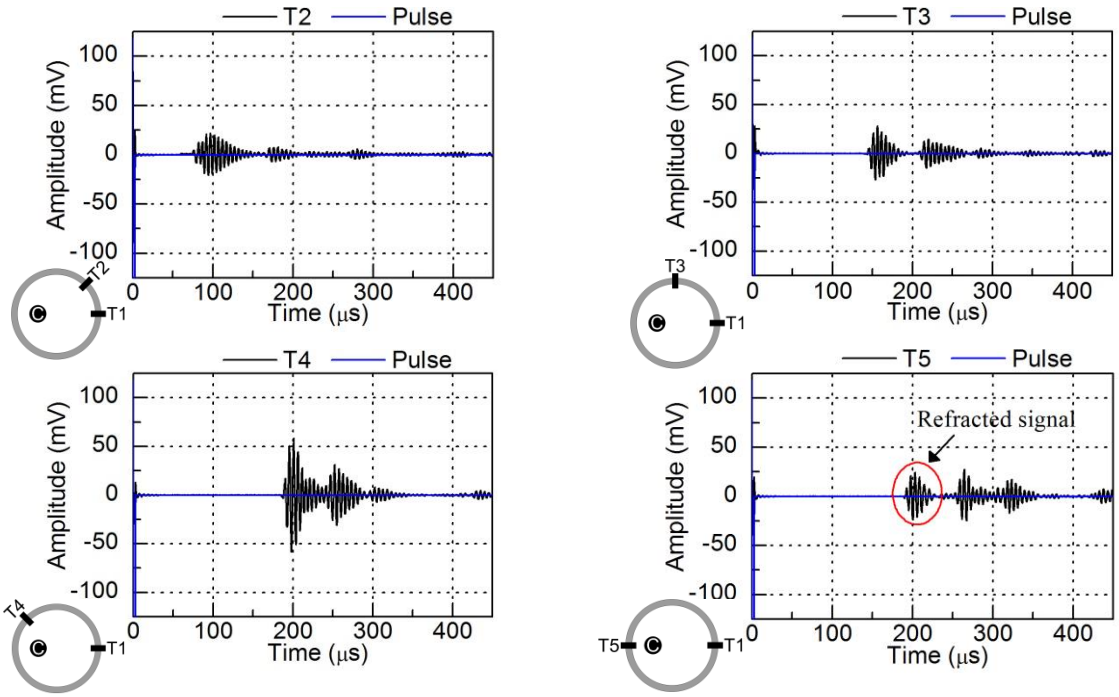

Position C

Figure 8: Recorded signals with phantom at position C.

Figure 9 shows the recorded signals when the phantom was placed at the position D, the signal that suffers influence of the phantom is T4, resulting on its attenuation whereas the signals of T2, T3, and T5 have almost the same response compared with no phantom (Fig. 5). Therefore, through T4 signal, the influence of the placement of the phantom can be seen on the measured signal.

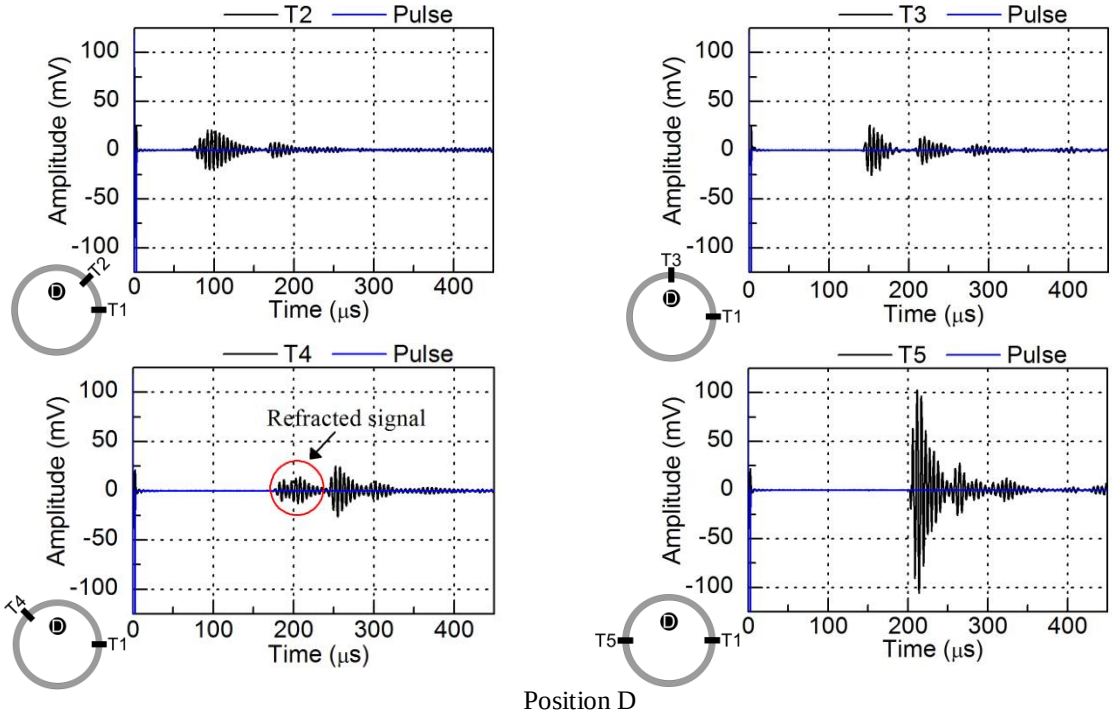

Figure 9: Recorded signals with phantom at position D.

4. CONCLUSION

The development of an experimental test bench for UST system was presented. The manufactured transducers presented resonance frequencies below 200 kHz with amplitudes between 20 and 300 mV_{PP}. The difference in amplitude response is mainly given by the matching layer, which depends on its thickness and mixture proportion. Thus, manufacturing process of the matching layer needs to be improved.

The system can record signals reflected and refracted from the wooden cylinder wall and the phantom, and the differences in the signals when the phantom is placed in different positions inside the test bench can be observed. As next step, an electronic system will be developed, acoustic pressure generated by the transducers will be measured by a hydrophone, sensitivity of each transducer will be measured, and algorithms for UST imaging will be developed to recreate phantom images.

5. ACKNOWLEDGEMENTS

This work is supported by grant #133845/2018-4, Conselho Nacional de Desenvolvimento Científico e Tecnológico (CNPq), and grant #2018/00710-1, São Paulo Research Foundation (FAPESP).

6. REFERENCES

Ball, L., Vercesi, V., Costantino, F., Chandrapatham, K. and Pelosi, P., 2017. "Lung imaging: how to get better look inside the lung". *Annals of translational medicine*, v. 5, p. 294.

Chiumello, D., Froio, S., Bouhemad, B., Camporota, L. and Coppola, S., 2013. "Clinical review: Lung imaging in acute respiratory distress syndrome patients - an update". *Critical Care*.

Cinel, I., Jean, S. and Dellinger, R. P., 2007. *Dynamic Lung Imaging Techniques in Mechanically Ventilated Patients*. Springer, Berlin, Heidelberg.

Coelho, B. S. and PAI, C. N., 2017. "Manufacturing of Multi-Element Piezoelectric Transducer for use in Ultrasound Elastography". In *Proceedings of the 24nd International Congress of Mechanical Engineering - COBEM 2017*. Curitiba, Brazil.

Kunkel, H. A., Locke, S. and Pikeroen, B., 1990. "Finite-element analysis of vibrational modes in piezoelectric ceramic disks". *IEEE Transactions on Ultrasonics, Ferroelectrics and Frequency Control*, v. 37, p. 316-328.

Liu, C., Xue, C., Zhang, B., Zhang, G. and He, C., 2018. "The Application of an Ultrasound Tomography Algorithm in a Novel Ring 3D Ultrasound Imaging System". *Sensors*, v. 18.

Nieman, G. F., Satalin, J., Andrews, P., Aiash, H., Habashi, N. M. and Gatto, L. A., 2017. "Personalizing mechanical ventilation according to physiologic parameters to stabilize alveoli and minimize ventilator induced lung injury (VILI)". *Intensive care medicine experimental*.

Polese, G., Serra, A. and Rossi, A. N., 2005. "Respiratory mechanics in the intensive care unit". *ERS Journals*.

Rueter, D., Hauber, H.P., Droeman, D., Zabel, P. and Uhlig, S., 2009. "Low-Frequency Ultrasound Permeates the Human Thorax and Lung: a Novel Approach to Non-Invasive Monitoring". *Ultraschall in der Medizin - European Journal of Ultrasound*.

Song, X., Li, M., Yang, F., Xu, S. and Abubakar, A., 2018. "Feasibility study of acoustic imaging for human thorax using an acoustic contrast source inversion algorithm". *The Journal of the Acoustical Society of America*.

Steiner, G., Soleimani, M. and Watzenig, D., 2008 "A bio-electromechanical imaging technique with combined electrical impedance and ultrasound tomography". *Physiological Measurement*.

7. RESPONSIBILITY NOTICE

The authors are the only responsible for the printed material included in this paper.